Crystal Structure and Magnetic Behaviour of Vanadium Doped Strontium Cobaltate

Manoj Prajapat[1, 2, b)], Sourav Marik[1], K Santhosh Kumar[1], R. P. Singh[1], D. S. Rana[1] and Vilas Shelke[2, a)]

[1]*Department of Physics, Indian Institute of Science Education and Research (IISER) Bhopal, Madhya Pradesh, 462066, India*
[2]*Novel Materials Research Laboratory, Department of Physics, Barkatullah University, Bhopal 462026, M.P., India*
[a)]drshelke@gmail.com
[b)] manojsop88@gmail.com

Abstract: Herein, we report the structural and magnetic properties of polycrystalline $SrCo_{1-x}V_xO_{3-\delta}$ (x = 0.05 and 0.1) samples. Room temperature x-ray diffraction analysis shows "314 – type" tetragonal structure (S. G.: I4/mmm) with a $2a_p \times 2a_p \times 4a_p$ type unit cell. The micron size particles with triangular shapes were observed in morphology studies by the scanning electron microscopy. The weight losses observed from the thermogravimetric analyzer for x = 0.05 and 0.1 were ~ 0.75% and ~ 15% respectively. The Fourier transform infrared spectroscopy of symmetric and asymmetric stretching vibrational modes were studies in the 400-4000 cm^{-1} region. The magnetic susceptibility reveals that the materials exhibited ferrimagnetic-type transition above room temperature (359 K and 364 K for x = 0.05 and x = 0.1 respectively). These results, can approach to design of gas sensors or cathode materials.

INTRODUCTION

Cobalt oxides have attracted immense interest in recent times due to their different oxidation states (Co^{2+}, Co^{3+}, and Co^{4+}) and complex interactions among them [1]. There are three various spin states exists for Co^{3+}, two of them are magnetic with high – spin state (HS, $t_{2g}^4e_g^2$, S = 2) and intermediate - spin state (IS, $t_{2g}^5e_g^1$, S = 1) and remaining is non-magnetic with low spin state (LS, $t_{2g}^6e_g^0$, S = 0). Co^{4+} can also exists in two magnetic spin states as HS (HS, $t_{2g}^4e_g^1$, S = 1.5) and LS (LS, $t_{2g}^5e_g^0$, S = 0.5). Among the perovskite family, $SrCoO_{3-\delta}$ shows different magnetic spin ordering such as ferro, antiferro, ferri due to presence of two mixed Co valence states (Co^{3+}, CO^{4+}) and complex interaction between them leads to exchange bias properties [2]. In addition, $SrCoO_{3-\delta}$ perovskite shows the diverse properties depending on the synthesis temperature and method, doping element and oxygen deficiency as per the literature of (*Ln*, Sr)$CoO_{3-\delta}$(*Ln* = La, Nd, Dy) [3], $SrCo_{1-x}V_xO_{3-\delta}$and Sr(R, Co)$O_{3-\delta}$(Fe, Mn, and Ru)[2, 4-7]. Among all of them, $SrCoO_3$ perovskite with cubic structure forms at high temperature (typically above 900 ˚C) and under high oxygen pressure shows the ferromagnetic ordering near room temperature [3]. Also, oxygen deficiency in parent compound forms in various structures such as hexagonal, tetragonal and Brownmillerite type [3, 7]. In addition, technical point of view it has diverse applications such as in the area of spintronics and solid state chemistry (solid oxide fuel cells, gas sensor and catalysis) [8-9].

Herein, we have reported the microstructure by x-ray diffraction and Fourier transform infrared spectroscopy, structural morphology by scanning electron microscope and magnetic properties in V^{5+} ion doped $SrCo_{1-x}V_xO_{3-\delta}$(x = 0.05, 0.10, and 0.15).

EXPERIMENTS

Polycrystalline samples $SrCo_{1-x}V_xO_{3-\delta}$(x = 0.05, 0.10, and 0.15) were prepared by conventional solid state reaction method using stoichiometric amounts of $SrCO_3$ (99.9%), Co_3O_4 (99.95%), and V_2O_3 (99.99%) [10]. Room temperature x-ray diffraction (RT-XRD) measurements were carried out using PANalytical Bragg–Brentano Cu-Kα_1 (λ = 1.540598 Å) diffractometer. Scanning electron microscope (SEM) was used to obtain the morphological aspects of the powder samples.The thermal decomposition processes of the precursor powder samples were studied by thermogravimetric analyses (TGA) using Perkin Elmer Pyris 6 TGA-4000 at a heating rate of 10 ˚C min^{-1} in N_2 at 20 ml min^{-1}. The Fourier transform infrared (FTIR) spectra were recorded using FT-

IR Perkin-Elmer spectrometer. The magnetization measurements were performed using a superconducting quantum interference device vibrating sample magnetometer (SQUID-VSM, Quantum Design MPMS3).

RESULTS AND DISCUSSION

Fig. 1(a) shows the RT-XRD pattern of $SrCo_{1-x}V_xO_{3-\delta}$(x = 0.05, 0.1 and 0.15) samples. The XRD data were used to check the phase purity and to calculate the average particle size of the samples. The indexing of the points in the diffraction pattern was done using "314 - type" tetragonal structure(space group: I4/mmm) with $2a_p \times 2a_p \times 4a_p$($a_p$ = cell parameter of the perovskite unit cell) type unit cell.

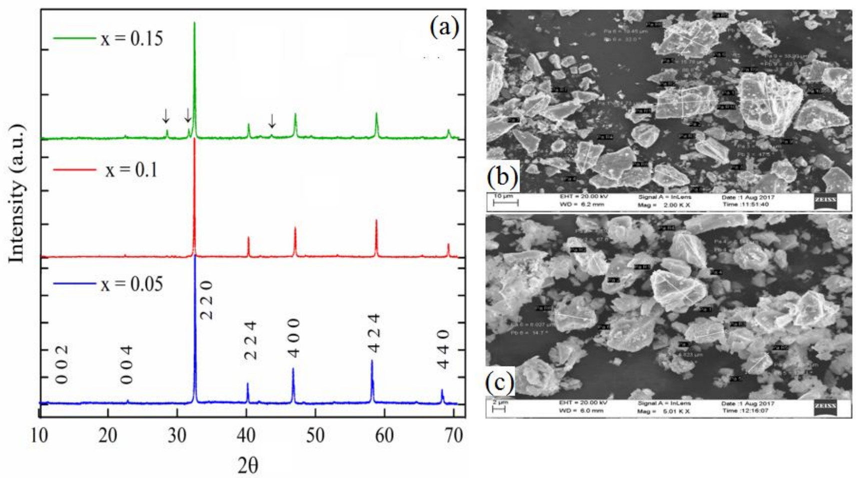

FIGURE 1.(a) Shows RT-XRD for $SrCo_{1-x}V_xO_{3-\delta}$ (x = 0.05, 0.1, 0.15) and secondary phase indicated by '↓'.Structural morphology forx = 0.05 and 0.10 shown in (b) and (c) respectively.

The calculated average lattice parameters area_{avg} = b_{avg} = 7.524 Å and c_{avg} = 15.5316 Å. However, the secondary phases started to appear for x> 0.1 and atx = 0.15, the tetragonal main phase with other minor phase indicated was shown by '↓' in Fig.1 (a). Therefore, the solubility limit of V^{5+} ion [6] in the $SrCo_{1-x}V_xO_{3-\delta}$system is 10%. We have calculated the tolerance factor to justify the crystal system. The tolerance factor, *t,* defined by

$$t = \frac{r_A + r_O}{\sqrt{2}(r_B + r_O)}, \tag{1}$$

where, r_A,r_B, and r_O are ionic radii of each atoms. The calculated value of tolerance factor for $SrCo_{1-x}V_xO_{3-\delta}$ is 1.02, also suggests the system crystallizes in the tetragonal (t> 1) symmetry. To obtain the crystalline size (L_{hkl}), we have used the Scherrer's formula,

$$L = \frac{0.9\,\lambda}{\beta\, cos\theta}, \tag{2}$$

where, L_{hkl}, λ, □, and θ are the crystallite size, wavelength of x-rays, full width half maxima and the Bragg's angle respectively. The broadening in peak at higher d-spacing of crystal plane in x-ray diffraction is play a promising role to calculate the particle size. The crystallite size calculated at RT is lies in the range of 45–144 nm and the average crystallite size, L_{hkl}~ 72.24 nm and ~ 91.41 nm for x = 0.05 and x = 0.1 respectively. A noticeable crystallite size increase with increasing value of x in polycrystalline $SrCo_{1-x}V_xO_{3-\delta}$ samples.

Further information about the formation of particle size, shape and distributions of particles, we carried out the surface morphology measurements on polycrystalline $SrCo_{1-x}V_xO_{3-\delta}$ samples using SEM. Both the samples reveled particles with various shapes, size and irregular distribution as shown in Fig.1(b) and (c). The morphology shows that particles formed in triangle shape, which is highlighted in Fig.1(b) and (c). The average particle size obtained from the SEM measurements are in the range of 5-20 µm for both the samples.

Fig.2 (a) shows the thermos-decomposition for $SrCo_{1-x}V_xO_{3-\delta}$ (x = 0.05 and 0.10) samples investigated by TGA in N_2. The temperature dependent weight loss profile conforms the apparent decomposition exhibited in both the sample. For x = 0.05, we have observed a minor weight loss up to ~ 0.5%. Whereas, for x = 0.1, it shows a gradual weight loss ~ 15% in the temperature range 30 – 900 ˚C. The decreasing in weight loss could be due to removal of H_2O and CO_2 molecules from the powder surface. The results clearly indicates that with increasing V^{5+} doping surface reaction with of H_2O and CO_2 molecules increase which can be useful in design of gas sensors or cathode materials.

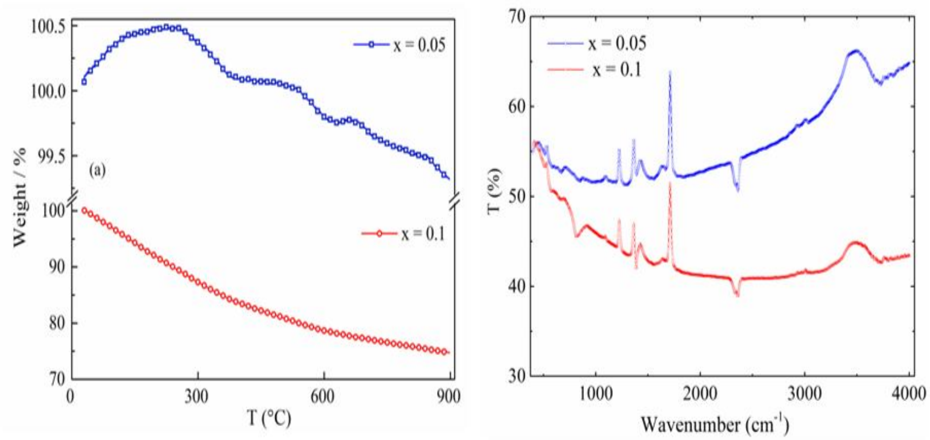

FIGURE2. (a) TGA curve shows weight loss (%) as a function of temperature and (b) Infrared spectra for $SrCo_{1-x}V_xO_{3-\delta}$ samples.

In infrared regions, vibration frequency is important to control the properties and development process of materials. The room temperature FTIR spectroscopy spectra of $SrCo_{1-x}V_xO_{3-\delta}$ (x = 0.05 and 0.10) samples are shown in Fig.2 (b). Since, the M-O (M = Co, Sr, V) bands exhibited in various vibration mode, for instance, Co-O exhibits vibration modes depending on the different valence Co^{2+}, Co^{3+}, and Co^{4+}. The absorption bands at 580 cm^{-1} and 670 cm^{-1} are attributed to the Co-O asymmetric stretching vibrational mode with different valance Co^{3+} (octahedral coordinated) and Co^{2+} (tetrahedral coordinated) respectively [11]. The asymmetric stretching bands at 421 cm^{-1} and 512 cm^{-1} at lower frequency regions are possibly due to the M-O groups (M = Co, Sr and V) [11, 12]. The $SrCo_{1-x}V_xO_{3-\delta}$composition exhibits intense bands between 1000 - 1800 cm^{-1} (at 997 cm^{-1},1159 cm^{-1}, 1389 cm^{-1} and 1560 cm^{-1}) due to stretching vibration mode of V-O and V-O-V type as reported in previous studies [2, 13]. The absorbance peak at higher frequency regions (2945 cm^{-1}, 3035 cm^{-1},3135 cm^{-1}) are difficult to assign in the FTIR.

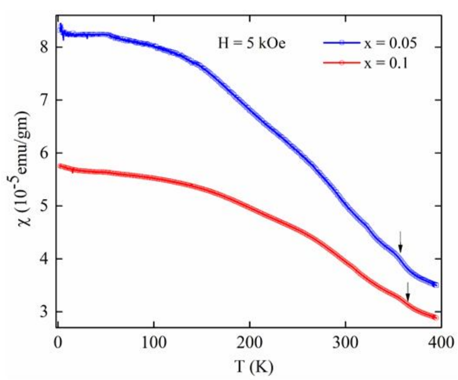

FIGURE3.Temperature dependent field cooled susceptibility for $SrCo_{1-x}V_xO_{2.65\pm\delta}$ samples: x = 0.05 (red colour) and x = 0.10 (blue colour) and $T_c$indicated by'↓'.

The temperature dependent field cooled susceptibility (χ) measured at an applied magnetic field 5 kOe for both the samples were shown in Fig. 3. The behavior of χ suggest the ferrimagnetic-type transition at T_C= 359 K and 364 Kfor x = 0.05 and x = 0.1 respectively. Ferrimagnetic type transition well above the room temperature present in the system could be due to the antiferromagnetic alignment of the alternating high- spin (HS, $t_{2g}^4e_g^2$, S = 2) state and intermediate - spin (IS, $t_{2g}^5e_g^1$, S = 1) state of Co^{3+} [1, 10]. Also, an increase in the χ at low temperature indicates the complex magnetic interactions present in the system. However, we also observed that the decrease in magnetization with increasing the doping of non-magnetic V^{5+} ions [6].

CONCLUSION

The polycrystalline $SrCo_{1-x}V_xO_{3-\delta}$ (x = 0.05 0.1 and 0.15) perovskite oxides were prepared by solid state reaction method. RT-XRD analysis reveals that all the samples crystallizes in tetragonal symmetry with an average crystallite size 45-114 nm. The morphology of the compounds shows triangle shape of particles with various dimensions. TGA reveals the reactive nature of the sample with increasing V^{5+} concentration indicates that these materials are useful to develop new cathode materials or gas sensors. FTIR measurements are consistent with structure observed by RT-XRD measurement. The temperature dependent magnetic susceptibility behavior shows the ferromagnetic-type transition above room temperature in both the samples.

ACKNOWLEDGMENT

D. S. R., thanks the Science and EngineeringResearch Board (SERB), Department of Science and Technology, New Delhi, for financial support under research Project No. EMR/2016/003598.

REFERENCES

1. T. Motohashi, V. Caignaert, V. Pralong, M. Hervieu, A. Maignan, and B. Raveau, Phys. Rev. B **71**, 214424 (2005).
2. P. Mohanty, S. Marik, D. Singh, and R. P. Singh, Appl. Phys. Lett. **111**, 022402 (2017).
3. L. Xie, H. L. Huang, and Y. L. Lu, AIP Advance, **7**, 015207 (2017).
4. C. K. Xie, Y. F. Nie, B. O. Wells, J. I. Budnick, W. A. Hines, and B. Dabrowski, Appl. Phys. Lett. **99**, 052503 (2011).
5. M. James, M. Avdeev, P. Barnes, L. Morales, K. Wallork, R. Withers, J. of Solid State Chem. **180**, 2233-2247 (2007).
6. V. Cascos, L. Troncoso, J. A. Alonso Int. J. Hydrogen Energy **40**, 11333-1134 (2015).
7. N. E. Trofimenko, J. Paulsen, H. Ullmann, R. Müller, Solid State Ion. **100**, 183 (1997).
8. F. C. Chou, J. H. Cho, and Y. S. Lee, Phys. Rev. B **70,** 144526 (2004).
9. S. Roy, I. S. Dubenko, M. Khan, E. M. Candon, and N. Ali, Phys. Rev. B **71**, 024419 (2005).
10. S. Marik, M. Chennabasappa, J. F. Sanjulián, E. Petit, and O. Toulemonde, Inorg. Chem. **55**, 9778 (2016).
11. Y. Liu, G. Zhu, B. Ge, H. Zhou, A. Yuan, X. Shen, Cryst. Eng. Comm. **14**, 6264-6270 (2012).
12. S. Makhloufi, M. Omari, J. InorgOrganometPolm. **26**, 32-40 (2016).
13. A. Baranauskas, D. Jasaitis, A. Kareiva, Vibr. Spectrosc. **28**, 263 (2002).